

Journal Pre-proof

Efficient improvement for dissociation behavior and thermal decomposition of manganese ore by microwave calcination

Kangqiang Li, Jin Chen, Jinhui Peng, Mamdouh Omran, Guo Chen



PII: S0959-6526(20)31121-5

DOI: <https://doi.org/10.1016/j.jclepro.2020.121074>

Reference: JCLP 121074

To appear in: *Journal of Cleaner Production*

Received Date: 3 August 2019

Revised Date: 9 March 2020

Accepted Date: 11 March 2020

Please cite this article as: Li K, Chen J, Peng J, Omran M, Chen G, Efficient improvement for dissociation behavior and thermal decomposition of manganese ore by microwave calcination, *Journal of Cleaner Production* (2020), doi: <https://doi.org/10.1016/j.jclepro.2020.121074>.

This is a PDF file of an article that has undergone enhancements after acceptance, such as the addition of a cover page and metadata, and formatting for readability, but it is not yet the definitive version of record. This version will undergo additional copyediting, typesetting and review before it is published in its final form, but we are providing this version to give early visibility of the article. Please note that, during the production process, errors may be discovered which could affect the content, and all legal disclaimers that apply to the journal pertain.

© 2020 Published by Elsevier Ltd.

Author Contributions Section

Prof. Guo Chen, Prof. Jin Chen and Prof. Jinhui Peng conceived and designed the study. Prof. Jinhui Peng, Dr. Mamdouh Omran and Prof. Guo Chen performed the experiments. Prof. Guo Chen provided the raw materials, and Prof. Jinhui Peng provided the box-type microwave high temperature furnace. Mr. Kangqiang Li and Prof. Jin Chen wrote the paper. Dr. Mamdouh Omran and Prof. Guo Chen reviewed and edited the manuscript. All authors read and approved the manuscript.

Efficient improvement for dissociation behavior and thermal decomposition of manganese ore by microwave calcination

Kangqiang Li ^a, Jin Chen ^{a, **}, Jinhui Peng ^{a, b}, Mamdouh Omran ^c, Guo Chen ^{a, b, *}

^a *Faculty of Metallurgical and Energy Engineering, Kunming University of Science and Technology, Kunming 650093, P.R. China.*

^b *Key Laboratory of Green-Chemistry Materials in University of Yunnan Province, Yunnan Minzu University, Kunming 650500, P.R. China.*

^c *Process Metallurgy Research Group, Faculty of Technology, University of Oulu, Finland.*

* Corresponding author: Tel: +86-871-65138997; Fax: +86-871-65138997

E-mail address: guochen@kust.edu

** Co-Corresponding author: Tel: +86-871-65138997; Fax: +86-871-65138997

E-mail address: jinchen@kust.edu.cn

Abstract:

Traditional smelting process of manganese ore was plagued with high consume of power and coke, and spraying and slag turning accidents caused by violent decomposition of carbonates and manganese oxides in manganese ore. In the present work, the thermal decomposition mechanism and phase structures of manganese ore were systematically investigated, calcined through microwave calcination approach and characterized by XRD, SEM and EDAX. Results indicated that microwave calcination had a significantly better effect than conventional calcination for manganese ore. An increase in calcination temperature was found to present a more profound effect than calcination duration. The optimum calcination temperature was identified to be 950 °C, with the calcination duration being 30 min, and manganese ore grade increased from initial 30% to 39%-42%, with the pulverization ratio being 8%-9%. Peak intensities of Mn_3O_4 phase enhanced with calcination temperature increasing, and irregular cracks and pits appeared on the surface of the microwave calcined manganese ore. Meanwhile, the feasibility of decomposition reactions of manganese ore at the considered temperature regime was confirmed by thermodynamics analysis. The upgrading and modified manganese ore by microwave calcination can realize the direct smelting of the concentrate. The work proposes an efficient calcination idea for manganese ore by microwave calcination.

Keywords: manganese ore; microwave calcination; phase structure; thermal decomposition; dissociation behavior

1 Introduction

As an important strategic mineral resource, manganese ore relates to social and economic development, which has been widely applied as deoxidizers, desulfurizers and alloying agents in the steel manufacturing (Barik et al., 2017; Wang et al., 2018; Zeng et al., 2018; Zhang et al., 2017); additionally, its far extensive applications include electrode materials, magnetic materials, building materials and catalysts (He et al., 2017; Meshram et al., 2017; Rifat et al., 2018; Saleh et al., 2017). However, the presence of contaminants such as adsorbed water, molecular water and high-valence oxides, causes the smelting process to be energy intensive and large coke consumption, even with unstable furnace conditions (Kralj et al., 2015; Su et al., 2012; Zhao et al., 2014). Additionally, the presence of gases formed by the decomposition of carbonates, high-valence manganese oxides and crystal water, results in accidental spraying and slag turning, rendering serious safety issues in the manufacturing process (Adewale et al., 2016; Jeswani and Azapagic, 2012). As a consequence of such issues, manganese ore cannot be directly smelted into the furnace, hampering its industrial continuous production. As a recent development, rotary kiln is applied to calcine manganese ore by domestic manganese alloy manufacturers with good effect, however the wide spread adoption of rotary kiln is hampered by patent protection (Kang et al., 2011). Meanwhile, “reduction, resource utilization and reuse” of manganese ore is urgently to be solved for manganese ore resources industries, especially the efficient recycling of manganese ore resources, clean production, and the harmless treatment of waste, far away the requirements of economic development. The current technical problems mainly represents as follows: it's difficult to efficiently use low-grade manganese ore resources; high levels of harmful

elements such as sulfur (S) and phosphorus (P) render it difficult to develop and utilize; serious phenomenon about mining rich mines and abandoning poor mines results low comprehensive utilization; weak system research on theory, process and equipment leads to large resources and energy consumption, serious ecological damage and environmental pollution; backward harmless treatment technology for “three wastes” with large waste emissions (Guo et al., 2013). Hence, it necessitates the development of better calcination technologies for manganese ore so as to overcome those shortcomings.

Microwave heating as a novel and green heating method, has been found increasingly frequent in the comprehensive utilization of manganese ore (Chen et al., 2016; Li et al., 2019a; Li et al., 2020a), even extended to “three waste” treatment and ceramics material synthesis (Chen et al., 2020; Li et al., 2020b; Li et al., 2020c). The essence of microwave heating is the process in which the required energy is directly transferred to the reacting molecules or atoms inside the material, and microwave energy is converted into heat energy through the dielectric loss of the material, followed by producing a thermal effect to cause the material to be heated (Hou et al., 2019; Li et al., 2019b; Li et al., 2019c; Liew et al., 2019). Meanwhile, attributed to the difference of the electromagnetic properties of various minerals, this energy conversion method makes it possible to preferentially heat the useful minerals rather than the gangue in the ore, resulting in uneven distribution of temperature in the multi-phase complex ore system and causing thermal stress between the useful mineral and the ore interface, further promoting the dissociation between useful minerals and gangue (Cheng et al., 2019; Hou et al., 2019; Li et al., 2020d; Li, et al., 2019); meanwhile, the interfacial area and diffusional rates increase, with the accelerated chemical reactions and effective separation of valuable elements from the

inclusion minerals (Allamia et al., 2019; Li et al., 2019; Ye et al., 2018a). Actually, Ye et al. utilized microwave calcination to achieve the selective carbothermal reduction of Mn_xO_y and Fe_xO_y in pyrolusite, with the formation of the loose and porous MnO phase and dense Fe_3O_4 phase (Ye et al., 2018b). Li et al. investigated the microwave-enhanced biomass pyrolysis reduction behavior of low-grade pyrolusite, and reported MnO product endowed good crystalline structures, having a loose and porous surface with numerous cracks and holes (Li et al., 2019a). Chen et al. applied microwave calcination to investigate the thermal decomposition and dissociation behavior of manganese ore, and reported that manganese ore could be rapidly heated to 1000 °C in 17 min by microwave calcination, with an increase of manganese content from 30 % to 40 % (Chen et al., 2016). Above literatures clearly indicate that microwave calcination replacing traditional calcination technologies offers the improved decomposition efficiency of manganese ore, with better thermal efficiency and shorter calcination duration; meanwhile, the microwave calcined manganese ore is upgraded and modified with irregular cracks and pits appeared on the surface, which may realize the direct smelting of the concentrate.

Currently, the efficient recycling of manganese ore resources, clean production, and the harmless treatment of waste are urgent to be realized for manganese ore resources industries. Moreover, previous work focused on the microwave-assisted grinding, drying, reduction, and oxidation roasting for manganese ore; in addition, Amankwah and Pickles have verified the feasibility of microwave irradiation on manganese ore, and highlighted that the manganese ore was a relatively good microwave absorber and the addition of a small percentage to the feed resulted in improved microwave coupling (Amankwah and Pickles, 2005). However, no

more detailed information was provided about effects of microwave calcination on the physical properties and phase structure of manganese ore, and the comparison between microwave calcination and conventional calcination, even the calcination mechanism of manganese ore. Towards which, in the present work, the beneficial effects of microwave calcination as a suitable efficient alternative on manganese ore was attempted to explore, and the decomposition mechanism of manganese ore by microwave calcination was investigated. Meanwhile, effects of calcination temperature and calcination duration on the weight loss, T_{Mn} content, pulverization ratio, crystal structures, and microstructure morphology of manganese ore were comparatively analyzed, with the raw manganese ore and the microwave calcined samples characterized by XRD, SEM and EDAX, and calcined through microwave calcination and traditional calcination process.

2 Materials and methods

2.1 Materials

Manganese ore utilized as the experimental raw material for the study, was provided by Dounan Manganese Industry Co., Ltd (Wenshan city, Yunnan Province, P.R. China). The chemical compositions of raw manganese ore were determined by Kunming Metallurgical Research Institute (Kunming city, Yunnan Province, P.R. China), and the analytical results were illustrated in Table 1. It was characterized from Table 1 that the Mn content of the manganese ore was 32.81%; the iron content was 1.52%, with the iron to manganese ratio of 21.87; and the phosphorus content was 0.072%, with the phosphorus to manganese ratio of 0.0022. The component analysis indicated the manganese ore was high-grade pyrolusite

($T_{Mn} \geq 30\%$) of low iron type and low phosphorus type.

2.2 Characterization

The crystal structures and microstructure morphology of raw manganese ore and the microwave calcined samples were analyzed by X-ray diffractometer (X'Pert³ powder, Panaco, Netherlands) and scanning electron microscopy (SEM, XL30ESEM-TMP, Philips, Holland); meanwhile, the energy dispersion scanner spectrometer (EDAX, USA) attached to the SEM instrument was utilized to determine the elemental compositions of the microwave calcined samples. Wherein the XRD patterns were recorded at a scanning rate of 1.6 °/min with 2-theta ranging from 10 ° to 90 ° using a diffractometer with CuK α Radiation ($\lambda=1.540598$ Å) and a PIXcel1D-medipix3 detector, with the anode current and voltage operated at 40 mA and 40 kV, respectively.

For the crystal structures of raw manganese ore, it can be summarized from Fig. 1(a) that the main phases of the manganese ore contained Mn₂O₃ (JCPDS: 65-7467), MnCO₃ (JCPDS: 44-1472), CaCO₃ (JCPDS: 70-0095), Ca(Mn, Mg)(CO₃)₂ (JCPDS: 83-1531), and SiO₂ (JCPDS: 86-1560). In addition, for the microstructure morphology of raw manganese ore, it was observed from Fig. 1(b) that the interface between the various phases of manganese ore was clear, Mn₂O₃, MnCO₃ and CaCO₃ phases were distributed in a band shape, meanwhile SiO₂ existed in dots laid in MnCO₃ phase. Raw manganese ore samples were brown-black, light aubergine, with alternative appearance of white bands. The brown-black band was mixed with manganese oxide and manganese carbonate; and the light aubergine band was mainly rhodochrosite; additionally, the white band was calcite. From the above analysis, it can be concluded that the manganese ore meets the characteristics of the braunite-carbonate

manganese ore.

2.3 Instrumentation

The calcination experiments of manganese ore were performed in a box-type microwave high temperature furnace (HM-X08-16). The schematic diagram of microwave high temperature furnace was illustrated in Fig. 2. As shown in Fig. 2, the microwave furnace mainly consisted of microwave reactor, rotation, motor, infrared thermocouple, insulating brick, vacuum pump, a weight measurement system, a computer control system, barometer, flowmeter, and gas generator. The static vacuum was less than or equal to 10 Pa. The protective gas was injected into the reactor cavity based on the experimental requirements. The temperature of sample was measured by an infrared thermocouple (Marathon Series, Raytek, USA), with a maximum service temperature of 1600 °C. Continuous controllable microwave power ranged from 0 kW-3 kW, achieving with two magnetrons at 2.45 GHz microwave frequency for different experimental demand.

2.4 Procedure

To decrease the influence of ore sample size on calcination experiments, the raw bulk manganese ore was grinded by ball mill, and screened to prepare experimental materials with a particle size regime from 80 mm to 180 mm. Followed by the grinded manganese ore was dried at 105 °C for 12 h in an electric blast drying oven (DHG9079A) for facilitating subsequent characterization analysis. The quadrangle sampling method was utilized to ensure the uniform sampling of each group of experiments. To investigate effects of calcination temperature and calcination duration on the physical properties and phase structure of manganese ore, the ore sample with 200.0 g mass was introduced into ceramic crucible and

calcined by the microwave furnace (HM-X08-16) and an electric resistance furnace (YFX9/16Q-YC), respectively, without protective gas injected into the reaction cavity. Meanwhile, the calcination temperature was set to vary from 550 °C, 650 °C, 750 °C, 850 °C, and 950 °C, and the calcination duration ranged from 10 min to 60 min, with 10 min as a variable node. After attaining the set calcination temperature and calcination duration, the calcined samples were removed and cooled to room temperature by oxygen insulation for subsequent characterization analysis. Each set of calcination experiments of manganese ore was repeated 3 times, and the experimental results were averaged and then the error analysis of the experimental data was conducted by Origin 8.5.

The greater the weight loss, the more thorough the decomposition reaction and better the calcination effect will be. The weight loss of manganese ore is defined as the following equation,

$$w = \frac{(m_0 - m)}{m_0} \times 100\% \quad (1)$$

where w is the weight loss rate of manganese ore; m_0 is the mass of raw manganese ore, with an initial value of 200.0 g; m is the mass of manganese ore after microwave calcination.

3 Results and discussion

3.1 Effect of calcination duration on the weight loss of manganese ore

Effects of calcination duration on the weight loss of manganese ore at 850 °C and 900 °C by microwave calcination were illustrated in Fig. 3. As presented in Fig. 3, the trends of weight loss with calcination duration were similar at 850 °C and 900 °C. The weight loss was 16.53% at 900 °C for 20 min, while it increased to only 19.82% at calcination duration of 60

min by utilizing microwave calcination. Calcination duration had a significant effect on the weight loss at the first 20 min of microwave calcination process, representing by a straight rise in the weight loss of manganese ore with duration time prolonging, whether the microwave calcination temperature was at 850 °C or 900 °C. While duration time was higher than 30 min, its effect was gradually changed to be slight. The increase of calcination duration contributed to the completion of the formation-decomposition reactions of MnCO_3 phase and CaCO_3 phase in manganese ore, wherein MnCO_3 phase and CaCO_3 phase were decomposed into corresponding oxides and carbon dioxide (CO_2), including MnO and CaO , rendering the decrease of the weight loss of manganese ore. In addition, the weight loss was only 12.35% at 900 °C for 20 min by conventional calcination, while it increased to 17.31% at calcination duration of 60 min (see Supplementary data). A one to one comparison of the microwave calcination with conventional calcination indicated that the calcination effect by utilizing microwave heating was far better than that by conventional heating. Compared the weight loss by microwave calcination at duration of 20 min with the weight loss by conventional calcination at duration of 50 min, the effectiveness of microwave calcination was strongly authenticated, with shorter calcination duration, lower calcination temperature and higher efficiency.

Moreover, it can be observed from Fig. 3 that effects of calcination temperature on the weight loss were observed to be more significant than that of calcination duration. It was evident from Fig. 3 that a weight loss of 16.76% was obtained at 850 °C for the duration of 50 min, compared with the weight loss of manganese ore obtained at 950 °C with the duration of only 20 min. The influence difference about calcination temperature and calcination duration

was attributed to the excellent microwave-absorbing properties of manganese ore (He et al., 2019; Li et al., 2019b), and the kinetics of decomposition reactions with temperature. The higher calcination temperature indicates the more required energy, supplied by microwave heating and absorbed by the metal and metal oxides in manganese ore. Meanwhile, MnCO_3 phase is decomposed at the temperatures regime of 176 °C-343.7 °C, and the decomposition reaction of CaCO_3 phase arises at 522 °C-886.1 °C. Therefore, increasing calcination temperature indicates the dynamics requirements of decomposition reactions of MnCO_3 phase and CaCO_3 phase meet, while increasing calcination duration ensures the completion degree of decomposition reaction at a specific temperature, further rendering the influence difference about calcination temperature and calcination duration.

3.2 Effects of microwave calcination temperature on T_{Mn} content and pulverization ratio of manganese ore

Influence of calcination temperature on manganese content and pulverization ratio of microwave calcined samples were plotted in Fig. 4. Manganese ore with high manganese content is required for the manganese alloys smelting process. Higher the manganese content, higher will be the yield, lower will be consumption, and better will be the quality. For the low carbon ferromanganese smelting process, the rational utilization of manganese ore demands manganese content to be greater than 40%; while for the high-carbon ferromanganese and manganese-silicon alloy process, the manganese content is required to be greater than 35%. The manganese ore provided by the factory having manganese content less than 30.00%, obviously fails to meet the industrial furnace standards. It was observed from Fig. 4 that the manganese content increased progressively with the improvement of microwave calcination

temperature. The manganese content increased from only 32.16% at 550 °C, to 39.82% at 850 °C, and to 42.03% at 950 °C, respectively. The increase of manganese content was ascribed to that increasing calcination temperature meet the dynamics requirements of decomposition reaction of MnCO_3 phase and CaCO_3 phase, further contributing to the completion degree of the formation-decomposition reactions of MnCO_3 phase and CaCO_3 phase in manganese ore. Wherein MnCO_3 phase was decomposed into carbon dioxide (CO_2) and corresponding oxide MnO at the temperatures regime of 176 °C-343.7 °C, followed by CaCO_3 phase was decomposed into carbon dioxide (CO_2) and corresponding oxide CaO at the temperatures regime of 522 °C-886.1 °C, further rendering the increase of the manganese content in manganese ore. Thus, the results confirmed the manganese content of manganese ore after microwave calcination met the requirement of furnace standard.

The manganese ore fed to the furnace should meet suitable particle size range which usually is between 5 mm-75 mm, and the proportion particles less than 3 mm should be less than 10%. Regardless of the type of calcination method, crushing and pulverization are integral part of the manganese ore calcination process. It can be seen from Fig. 4 that the pulverization was determined in the range of 8%-9% at temperatures higher than 750 °C, indicating the suitability of manganese ore after microwave calcination to meet the furnace standards. Compared with conventional resistance heating, microwave heating endows unique selective and volumetric heating characteristics. Based on the excellent heating characteristics, the microwave calcined samples presented a smaller particle size distribution (Li et al., 2019a; Li et al., 2020a). The same conclusion can also be obtained from the work, through the microwave calcined manganese ore compared to the ground manganese ore, with a particle

size ranging from 80 mm to 180 mm.

3.3 Phase transformation analysis

Fig. 5 showed the phase compositions of the calcined manganese ore under different microwave calcination temperatures with a duration time of 30 min. In comparison with the XRD pattern of raw material shown in Fig. 1(a), after calcined at 650 °C for a duration of 30 min, the diffraction peaks of MnCO_3 phase disappeared, however with the absence of the decomposition product MnO , indicating that the MnCO_3 completely decomposed to MnO at temperature below 650 °C, which was oxidized to Mn_2O_3 . And the diffraction peaks of Mn_3O_4 phase appeared in the calcined sample, which could be ascribed to the partial conversion of Mn_2O_3 into Mn_3O_4 . Meanwhile, compared with the calcined sample at 650 °C, the diffraction peaks of $\text{Ca}(\text{Mn,Mg})(\text{CO}_3)_2$ phase in the calcined sample at 850 °C disappeared, and the diffraction peaks of new CaO phase appeared, which was attributed to the decomposition reaction of $\text{Ca}(\text{Mn, Mg})(\text{CO}_3)_2$ phase. The intensity of CaCO_3 diffraction peaks was smaller compared with that at 650 °C, indicating that a large amount of CaCO_3 was decomposed and the decomposition product was crystalline CaO . At temperatures higher than 950 °C, the calcined sample was mainly composed of Mn_2O_3 , Mn_3O_4 , SiO_2 , CaO , and a small amount of CaCO_3 without decomposed. Compared with the calcined sample at 850 °C, the diffraction peak intensity of Mn_2O_3 and CaCO_3 phases at 950 °C successively became smaller, indicating that the decomposition reactions were still in progress, showing better calcination effect at 950 °C. The manganese ore powder calcined at 950 °C can meet the requirements of the manganese content (>40.00%) and pulverization ratio (<10.00%), with the manganese content of 43.01%, all of which meet the furnace standards. Therefore, it could be considered that the

optimum calcination temperature was 950 °C.

3.4 Physical structure characterization

SEM images and EDAX spectra of the two microwave calcined samples at 850 °C and 950 °C were displayed in Fig. 6, attempting to evaluate effects of microwave calcination on the physical structure and semi-quantitative chemical analysis of manganese ore, further to exactly determine the optimum calcination conditions.

From Fig. 6(a) and (c), the microwave calcined sample was observed to be uniform, less dense and un-sintered. The microwave calcined samples at 850 °C and 950 °C with the duration of 30 min, appeared with numerous irregular small cracks and pits, which was attributed to the electromagnetic properties difference of various minerals. Based on the excellent microwave-absorbing properties of metal oxides (He et al., 2019; Li et al., 2019b), which can be quickly heated to a higher temperature, while weak absorbing materials such as SiO₂ phase were difficult to heat, resulting in uneven distribution of temperature in the multi-phase complex ore system and causing thermal stress between the useful mineral and the ore interface, further promoting the dissociation of useful minerals and gangue, representing by the interfacial area and diffusional rates increase, and the accelerated chemical reactions and effective separation of valuable elements from the inclusion minerals, with those cracks appeared; meanwhile, under microwave calcination, carbon dioxide (CO₂) was formed by the decomposition reactions of MnCO₃ and CaCO₃ phases, and oxygen (O₂) was generated by the deoxygenation reaction of $6\text{Mn}_2\text{O}_3(\text{s})=4\text{Mn}_3\text{O}_4(\text{s})+\text{O}_2(\text{g})$, those gas also contributed to the formation of the microstructure of calcined manganese ore with pits.

In addition, fracture comparison of manganese ore after microwave calcination and

traditional calcination was provided in Supplementary data. The degree of fragmentation of manganese ore by utilizing microwave furnace was far more evident than the electric resistance furnace. The microwave calcined samples exhibited multiple lengths and strips with thick and thin cracks, while the conventional calcined samples had no obvious cracks (see Supplementary data). During microwave calcination process, Mn_2O_3 and MnCO_3 phases can be rapidly heated with good microwave-absorbing properties, while CaCO_3 and SiO_2 phases are hard to be heated with weak microwave-absorbing characteristics (He et al., 2019; Li et al., 2019b). It results in the development of a temperature gradient between the phases, and leads to development of thermal stress, contributing to the break in the grain boundary, further to cause the strip crack. On contrary, during traditional calcination process, the heat is radiated to the surface of the manganese ore, which gets conducted from exterior to the interior of the manganese ore; as a result of thermal driving force, which happens progressively and slowly, rendering the uniform calcination of the various phases of the manganese ore is processed more or less. Manganese ore will break only after Mn_2O_3 , MnCO_3 , and CaCO_3 phase are thermally decomposed, therefore there were absent of visible cracks. Moreover, the manganese ore with cracks and pits supplies good physical properties for the subsequent reduction and leaching process. Therefore, microwave calcination replacing conventional calcination endows a better effect for the pretreatment of manganese ore.

Fig. 6(b) and Fig. 6(d) presented that the elements of microwave calcined samples at 850 °C and 950 °C were mainly Mn, Si, and Al. It can be obtained from Fig. 6(d) that the peak intensity of element Mn was lower than that in Fig. 6(b), which was attributed to the

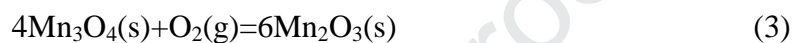
Mn₂O₃ phase was still in the process of getting converted to Mn₃O₄ phase. Moreover, the peak intensity of element O was higher than that in Fig. 6(b), which was attributed to the formation of CaO phase is produced by the decomposition reaction of CaCO₃ phase and the deoxygenation reaction of $6\text{Mn}_2\text{O}_3(\text{s})=4\text{Mn}_3\text{O}_4(\text{s})+\text{O}_2(\text{g})$, wherein the partial decomposition of Mn₂O₃ phase was decomposed into Mn₃O₄ phase. The EDAX results were in accordance with the XRD analysis for the calcined samples at 850 °C and 950 °C; therefore, it can be summarized that the optimum calcination temperature was 950 °C.

3.5 Calcination mechanism

The relationships between equilibrium constants and temperatures used for the formation-decomposition reactions of manganese ore were calculated and calibrated by thermodynamic software, including FactSage and HSC, and the thermodynamics graph was plotted in Fig. 7. The average atmospheric pressure of Kunming City (Yunnan, P.R. China) located in the Yunnan-Guizhou Plateau, being close to 0.08 Mpa; therefore, the partial pressure of CO₂ and O₂ in the air should be considered in the thermodynamics calculation for the decomposition reactions of manganese ore. From Fig. 7, it can be observed that the initial decomposition temperature of MnCO₃ phase was 176 °C, while the chemical boiling temperature was 343.7 °C; the initial decomposition temperature of CaCO₃ phase was 522 °C, while chemical boiling temperature was 886.1 °C; and the decomposition reaction of Mn₂O₃ phase arose at 577 °C-999.6 °C. Therefore, as depicted in Fig. 7, the thermodynamic feasibility of the decomposition reactions of manganese ore at the considered calcination temperature regime was clearly confirmed by thermodynamics analysis.

The XRD analysis shown in Fig. 5 indicated that the peak intensity of MnCO₃ phase

increased with the increase of calcination temperature, while the CaCO_3 phase in the microwave calcined samples gradually disappeared, however with an obvious increase in the peak intensity of Mn_3O_4 phase and CaO phase as decomposition products. Combined with XRD analysis, the formation-decomposition reaction of MnCO_3 phase and CaCO_3 phase could be summarized as following,



Calcination mechanism of manganese ore by microwave calcination could be expressed to obey the following order with temperature increasing: MnCO_3 phase was firstly decomposed at the temperatures regime of 176 °C-343.7 °C (Eq. (1)); followed by the decomposed product MnO phase was progressively oxidized to Mn_3O_4 and Mn_2O_3 phase (Eq. (2) and (Eq. (3))); then the decomposition reaction of CaCO_3 phase arose at 522 °C-886.1 °C (Eq. (4)); the initial decomposition temperature of Mn_2O_3 was 577 °C, wherein part of Mn_2O_3 was transformed into Mn_3O_4 (Eq. (5)). Observed from the XRD results in Fig. 5, Mn_3O_4 phase appeared at the calcination temperature of 650 °C and 950 °C, which corresponds to the temperature range of decomposition reaction of Mn_2O_3 at 577 °C-999.6 °C. Moreover, according to the Le Chatelier's principle, removing the gas product facilitates the decomposition reactions of manganese ore to proceed in the forward direction. Therefore, through the combination of thermodynamics and XRD patterns, it can be concluded that the

chosen optimum microwave calcination temperature at 950 °C was reasonable.

4 Conclusions

The following conclusions could be arrived based on the comparative analysis for crystal structures and microstructure morphology of raw manganese ore and microwave calcined samples, characterized by XRD and SEM. Results indicated that microwave calcination presented a significantly better effect than conventional calcination for manganese ore, with shorter calcination duration, lower calcination temperature and higher calcination efficiency. An increase in calcination temperature was found to present more profound effect than calcination duration. The manganese ore grade increased from initial 30% to 39%-42% and the pulverization ratio was 8%-9%, after calcined at 950 °C holding for 30 min, indicating suitability of manganese ore after microwave calcination to meet industrial furnace standards. Peak intensity of Mn_3O_4 phase increased with calcination temperature, which was ascribed to the decomposition reaction of MnCO_3 phase and the deoxygenation reaction of $6\text{Mn}_2\text{O}_3(\text{s})=4\text{Mn}_3\text{O}_4(\text{s})+\text{O}_2(\text{g})$. The surface of calcined manganese ore appeared irregularly with numerous small cracks and pits, wherein the pits were attributed to the release of gas by decomposition behavior of MnCO_3 phase and CaCO_3 phase, and the selective heating characteristic of microwave calcination rendered the formation of cracks. Thermodynamic analysis confirmed the thermodynamic feasibility of the manganese ore decomposition reactions by microwave calcination under the considered temperature regime in the present study, and driving the gas product of the decomposition reactions facilitated forward direction. The work confirms effective calcination for manganese ore with microwave calcination,

furthermore demanding further studies to explore the economic feasibility for commercial adoption.

Acknowledgments

Financial supports from the National Natural Science Foundation of China (No: U1802255), the Key Projects in the National Science & Technology Pillar Program during the Twelfth Five-year Plan Period (No. 2015BAB17B00), the Hunan Provincial Science and Technology Plan Project, China (No. 2016TP1007), and Innovative Research Team (in Science and Technology) in University of Yunnan Province were sincerely acknowledged.

Appendix A. Supplementary data

E-supplementary data for this work can be found in e-version of this paper online.

References

1. Adewale, R., Salem, D.J., Berrouk, A.S., Dara. S., 2016. Simulation of hydrogen production from thermal decomposition of hydrogen sulfide in sulfur recovery units. J. Clean. Prod. 112(5), 4815-4825. <https://doi.org/10.1016/j.jclepro.2015.08.021>.
2. Allamia, A.H., Tabasizadeha, M., Rohania, A., Farzada, A., Nayebzadehb, H., 2019. Precise evaluation the effect of microwave irradiation on the properties of palm kernel oil biodiesel used in a diesel engine. J. Clean. Prod. 241, 117777. <https://doi.org/10.1016/j.jclepro.2019.117777>.

3. Amankwah, R.K., Pickles, C.A., 2005. Microwave calcination and sintering of manganese carbonate ore. *Can. Metall. Quart.* 44(2), 239-247.
<https://doi.org/10.1179/cmqr.2005.44.2.239>.
4. Barik, S.P., Prabakaran, G., Kumar, L., 2017. Leaching and separation of Co and Mn from electrode materials of spent lithium-ion batteries using hydrochloric acid: Laboratory and pilot scale study. *J. Clean. Prod.* 147, 37-43.
<https://doi.org/10.1016/j.jclepro.2017.01.095>.
5. Chen, G., Li, L., Tao, C.Y., Liu, Z.H., Chen, N.X., Peng, J.H., 2016. Effects of microwave calcination on microstructures and structure properties of the manganese ore. *J. Alloy. Compd.* 657, 515-518. <https://doi.org/10.1016/j.jallcom.2015.10.147>.
6. Chen, J., Li, L., Chen, G., Peng, J.H., Srinivasakannan, C., 2016. Rapid thermal decomposition of manganese ore using microwave heating. *J. Alloy. Compd.* 699, 430-435. <https://doi.org/10.1016/j.jallcom.2016.12.379>.
7. Chen, G., Jiang, Q., Li, K.Q., He, A.X., Peng, J.H., Omran, M., Chen, J., 2020. Simultaneous removal of Cr(III) and V(V) and enhanced synthesis of high-grade rutile TiO₂ based on sodium carbonate decomposition. *J. Hazard. Mater.* 388, 122039.
<https://doi.org/10.1016/j.jhazmat.2020.122039>.
8. Cheng, S., Hu, W.H., Srinivasakannan, C., Xia, H.Y., Zhang, L.B., Peng, J.H., Zhou, J.W., Lin, G., Zhang, Q., 2019. Catalytic pyrolysis of the *Eupatorium adenophorum* to prepare photocatalyst-adsorbent composite for dye removal. *J. Clean. Prod.* 222, 710-721.
<https://doi.org/10.1016/j.jclepro.2019.03.103>.
9. Guo, Y.N., Xue, S.H., Li, H.B., Zou, T.X., 2013. Experimental study on rotary kiln for processing medium and low-grade manganese ore. *Min. Metall. Eng.* 33, 97-100.
<https://doi.org/10.3969/j.issn.0253-6099.2013.02.025>.

10. He, F., Chen, J., Chen, G., Peng, J.H., Srinivasakannan, C., Ruan, R., 2019. Microwave dielectric properties and reduction behavior of low-grade pyrolusite. *JOM*. 11, 3909-3914. <https://doi.org/10.1007/s11837-019-03522-8>.
11. He, H.P., Cao, J.L., Duan, N., 2017. Ultrasound and mechanical activation cleaner promote lattice manganese extraction: A combined experimental and modeling study. *J. Clean. Prod.* 143, 231-237. <https://doi.org/10.1016/j.jclepro.2016.12.124>.
12. Hou, K.X., Bao, M.L., Wang, L., Zhang, H., Yang, L., Zhao, H.T., Wang, Z.Y., 2019. Aqueous enzymatic pretreatment ionic liquid-lithium salt based microwave-assisted extraction of essential oil and procyanidins from pinecones of *Pinus koraiensis*. *J. Clean. Prod.* 236, 117581. <https://doi.org/10.1016/j.jclepro.2019.07.056>.
13. Hou, M., Guo, S.H., Yang, L., Ullah, E., Gao, J.Y., Hu, T., Ye, X.L., Hu, L.T., 2019. Microwave hot press sintering: New attempt for the fabrication of Fe-Cu pre-alloyed matrix in super-hard material. *Powder. Technol.* 356, 403-413. <https://doi.org/10.1016/j.powtec.2019.08.055>.
14. Jeswani, H.K., Azapagic, A., 2011. Water footprint: methodologies and a case study for assessing the impacts of water use. *J. Clean. Prod.* 19(12), 1288-1299. <https://doi.org/10.1016/j.jclepro.2011.04.003>.
15. Kang, G.Z., Jia, B.G., Wang, L.M., Shu, L., 2011. The use of rotary kiln in ferroalloys production. *Ferro-Alloys*. 42, 8-11. <https://doi.org/10.3969/j.issn.1001-1943.2011.03.003>.
16. Kralj, K.A., 2015. The re-usages of wastewater within industry: the positive impact of contaminants. *J. Clean. Prod.* 95, 124-130. <https://doi.org/10.1016/j.jclepro.2015.02.054>.
17. Li, K.Q., Chen, G., Chen, J., Peng, J.H., Ruan, R., Srinivasakannan, C., 2019a. Microwave pyrolysis of walnut shell for reduction process of low-grade pyrolusite. *Bioresour. Technol.* 291, 121838. <https://doi.org/10.1016/j.biortech.2019.121838>.

18. Li, K.Q., Chen, G., Li, X.T., Peng, J.H., Ruan, R., Omran, M., Chen, J., 2019b. High-temperature dielectric properties and pyrolysis reduction characteristics of different biomass-pyrolusite mixtures in microwave field. *Bioresource. Technol.* 294, 122217. <https://doi.org/10.1016/j.biortech.2019.122217>.
19. Li, K.Q., Chen, J., Chen, G., Peng, J.H., Ruan, R., Srinivasakannan, C., 2019c. Microwave dielectric properties and thermochemical characteristics of the mixtures of walnut shell and manganese ore. *Bioresource. Technol.* 286, 121381. <https://doi.org/10.1016/j.biortech.2019.121381>.
20. Li, K.Q., Chen, J., Peng, J.H., Ruan, R., Srinivasakannan, C., Chen, G., 2020a. Pilot-scale study on enhanced carbothermal reduction of low-grade pyrolusite using microwave heating. *Powder. Technol.* 360, 846-854. <https://doi.org/10.1016/j.powtec.2019.11.015>.
21. Li, K.Q., Chen, J., Peng, J.H., Ruan, R., Omran, M., Chen, G., 2020b. Dielectric properties and thermal behavior of electrolytic manganese anode mud in microwave field. *J. Hazard. Mater.* 381, 121227. <https://doi.org/10.1016/j.jhazmat.2019.121227>.
22. Li, K.Q., Chen, J., Peng, J.H., Koppala, S., Omran, M., Chen, G., 2020c. One-step preparation of CaO-doped partially stabilized zirconia from fused Zirconia. *Ceram. Int.* 46(5), 6484-6490. <https://doi.org/10.1016/j.ceramint.2019.11.129>.
23. Li, K.Q., Jiang, Q., Chen, J., Peng, J.H., Li, X.P., Koppala, S., Omran, M., Chen, G., 2020d. The controlled preparation and stability mechanism of partially stabilized zirconia by microwave intensification. *Ceram. Int.* 46(6), 7523-7530. <https://doi.org/10.1016/j.ceramint.2019.11.251>.
24. Li, L.Z., Chen, J., Wang, S., Tan, Y.D., Meng, B., Zou, G.F., Wang, F.M., Song, Z.L., Ma, H.Y., 2019. Utilization of biochar for a process of methane dry reforming coupled with steam gasification under microwave heating. *J. Clean. Prod.* 237, 117838. <https://doi.org/10.1016/j.jclepro.2019.117838>.

25. Li, S.M., Li, R.W., Tang, Y.N., Chen, G., 2019. Microwave-induced heavy metal removal from dewatered biosolids for cost-effective composting. *J. Clean. Prod.* 241, 118342. <https://doi.org/10.1016/j.jclepro.2019.118342>.
26. Liew, R.K., Chai, C., Yuh Yek, P.N., Phang, X.Y., Chong, M.Y., Nam, W.L., Su, M.H., Lam, W.H., Ma, N.L., Lam, S.S., 2019. Innovative production of highly porous carbon for industrial effluent remediation via microwave vacuum pyrolysis plus sodium-potassium hydroxide mixture activation. *J. Clean. Prod.* 208, 1436-1445. <https://doi.org/10.1016/j.jclepro.2018.10.214>.
27. Meshram, P., Somani, H., Pandey, B.D., Mankhand, T.R., Devecid, H., Abhilash, 2017. Two stage leaching process for selective metal extraction from spent nickel metal hydride batteries. *J. Clean. Prod.* 157, 322-332. <https://doi.org/10.1016/j.jclepro.2017.04.144>.
28. Saleh, T.A., Sulaiman, K.O., Al-Hammadi, S.A., Dafalla, H., Danmaliki, G.I., 2017. Adsorptive desulfurization of thiophene, benzothiophene and dibenzothiophene over activated carbon manganese oxide nanocomposite: with column system evaluation. *J. Clean. Prod.* 154, 401-412. <https://doi.org/10.1016/j.jclepro.2017.03.169>.
29. Rifat, F., Ravindra, R., Kamrul, H., Pravas, R.B., Veena, S., 2018. Thermal nanosizing: novel route to synthesize manganese oxide and zinc oxide nanoparticles simultaneously from spent Zn-C battery. *J. Clean. Prod.* 196, 478-488. <https://doi.org/10.1016/j.jclepro.2018.06.055>.
30. Su, W.N., Li, Q.H., Liu, Z.Y., Pan, C.H., 2012. A new design method for water-using network of multiple contaminants with single internal water main. *J. Clean. Prod.* 29-30, 38-45. <https://doi.org/10.1016/j.jclepro.2012.01.041>.
31. Wang, G.R., Zhang, J., Liu, L., Zhou, J.Z., Liu, Q., Qian, G.R., Xu, Z.P., Richards, R.M., 2018. Novel multi-metal containing MnCr catalyst made from manganese slag and

- chromium wastewater for effective selective catalytic reduction of nitric oxide at low temperature. *J. Clean. Prod.* 83, 917-924. <https://doi.org/10.1016/j.jclepro.2018.02.207>.
32. Ye, Q.X., Ru, J.J., Peng, J.H., Chen, G., Wang, D., 2018a. Formation of multiporous MnO/N-doped carbon configuration via carbonthermal reduction for superior electrochemical properties. *Chem. Eng. J.* 331, 570-577. <https://doi.org/10.1016/j.cej.2017.09.031>.
33. Ye, Q.X., Chen, J., Chen, G., Peng, J.H., Srinivasakannan, C., Ruan, R.S., 2018b. Effect of microwave heating on the microstructures and kinetics of carbothermal reduction of pyrolusite ore. *Adv. Powder. Technol.* 29(8), 1871-1878. <https://doi.org/10.1016/j.appt.2018.04.025>.
34. Zeng, G., Xian, J.W., Gourlay, C.M., 2018. Nucleation and growth crystallography of Al_8Mn_5 on B2-Al(Mn, Fe) in AZ91 magnesium alloys. *Acta. Mater.* 153, 364-376. <https://doi.org/10.1016/j.actamat.2018.04.032>.
35. Zhang, Y.T., Dan, Z.G., He, X.Y., Tian, Y., Wang, J., Qi, S.Y., Duan, N., Xin, B.P., 2017. Mn bio-dissolution from low-grade MnO_2 ore and simultaneous Fe precipitation in presence of waste electrolytic manganese anolyte as nitrogen source and iron scavenger. *J. Clean. Prod.* 158, 182-191. <https://doi.org/10.1016/j.jclepro.2017.04.129>.
36. Zhao, H.P., Su, W.N., Liu, Z.Y., 2014. Design of water-using networks of multiple contaminants with two internal water mains. *J. Clean. Prod.* 67, 37-44. <https://doi.org/10.1016/j.jclepro.2013.12.021>.

Table captions

Table 1 Chemical composition of raw manganese ore.

Figure captions

Fig. 1 XRD pattern (a) and SEM image (b) of raw manganese ore.

Fig. 2 Schematic diagram of microwave high temperature furnace.

Fig. 3 Effects of microwave calcination duration on the weight loss of manganese ore.

Fig. 4 Effects of microwave calcination temperature on T_{Mn} content and pulverization ratio of manganese ore.

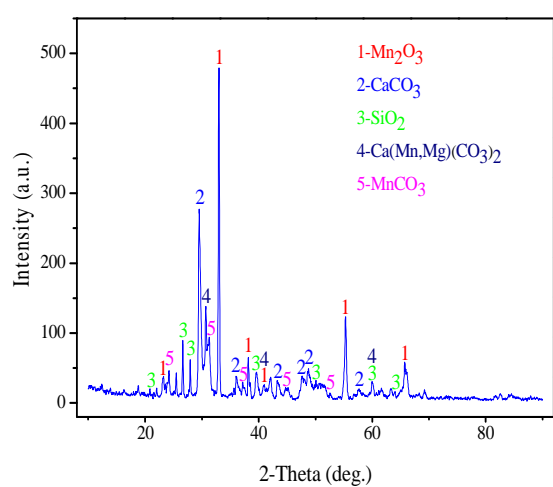
Fig. 5 XRD patterns of microwave calcined samples at different calcination temperatures.

Fig. 6 SEM images and EDAX spectra of microwave calcined samples, (a) SEM of the sample calcined at 850 °C for 30 min; (b) EDAX of spot 1; (c) SEM of the sample calcined at 950 °C for 30 min; (d) EDAX of spot 2.

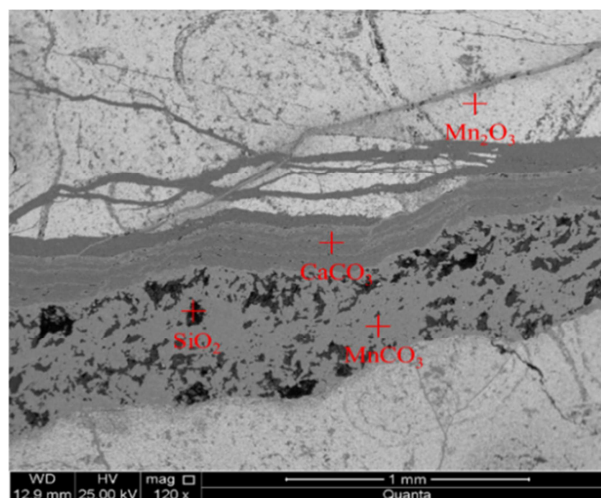
Fig. 7 Dependency of equilibrium constant on temperatures for the formation-decomposition reactions of manganese ore.

Table 1 Chemical composition of raw manganese ore

Compositions	T _{Mn}	T _{Fe}	SiO ₂	Al ₂ O ₃	CaO	MgO	TiO ₂
Mass/W%	32.81	1.52	18.23	1.96	19.87	1.76	0.38
Compositions	P	S	Pb	Zn	Ni	Co	Others
Mass/W%	0.072	17.88	0.89	1.35	0.053	0.021	3.204



(a)



(b)

Fig. 1 XRD pattern (a) and SEM image (b) of raw manganese ore.

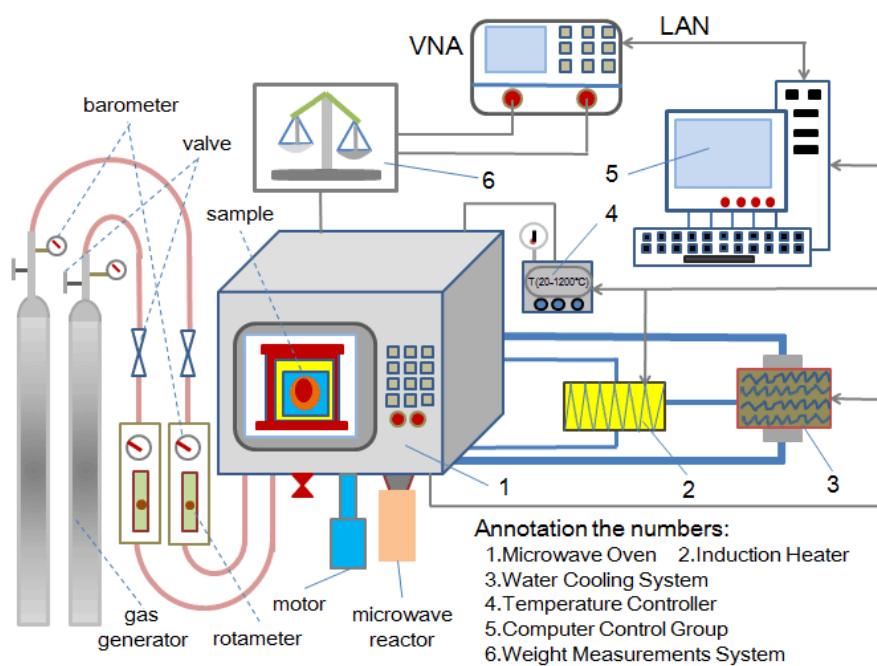


Fig. 2 Schematic diagram of microwave high temperature furnace.

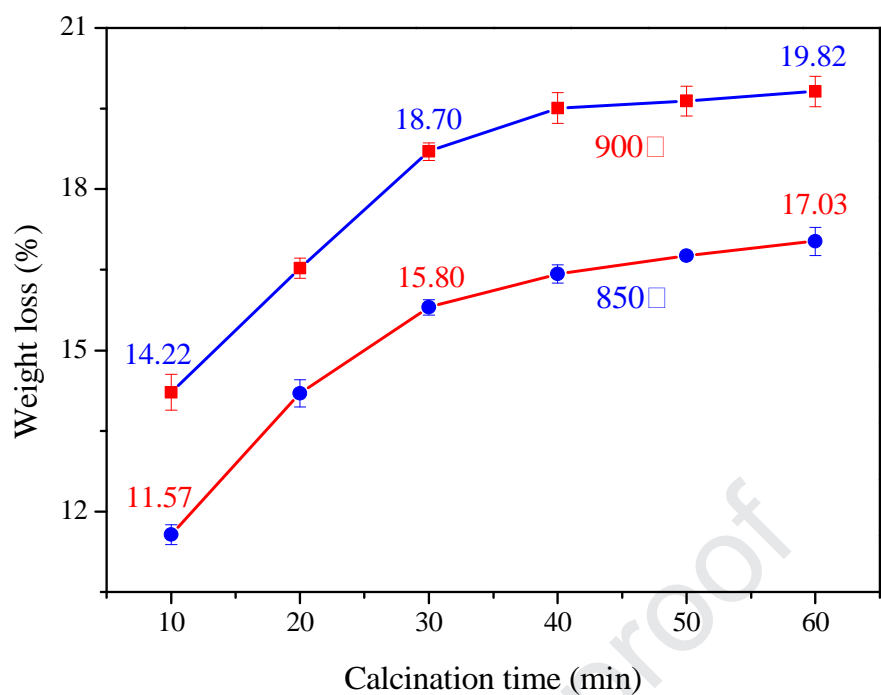


Fig. 3 Effects of microwave calcination duration on the weight loss of manganese ore.

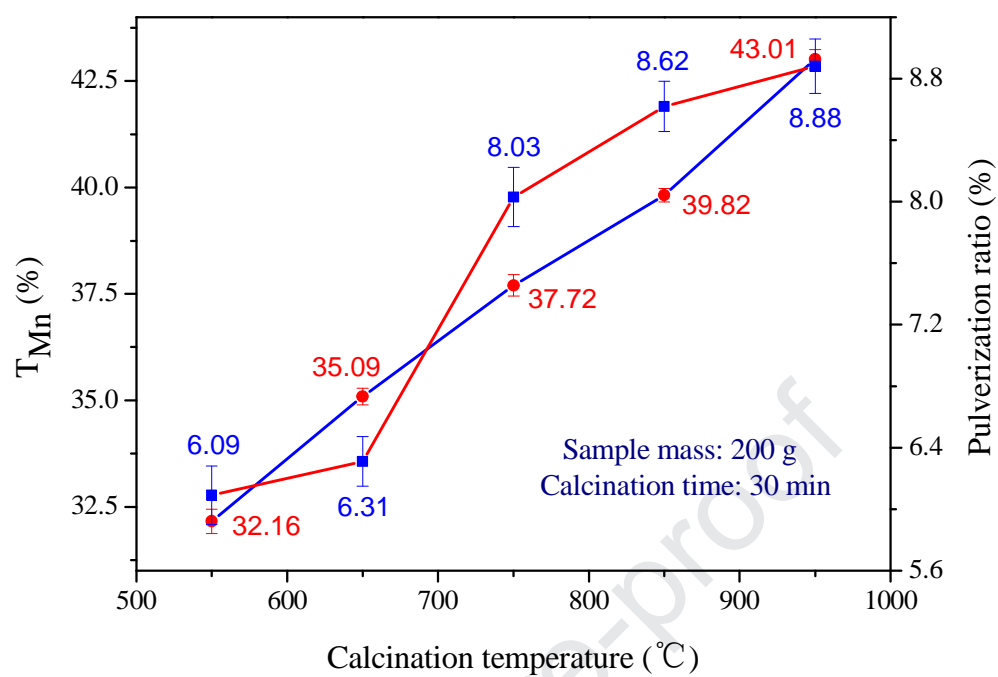


Fig. 4 Effects of microwave calcination temperature on T_{Mn} content and pulverization ratio of manganese ore.

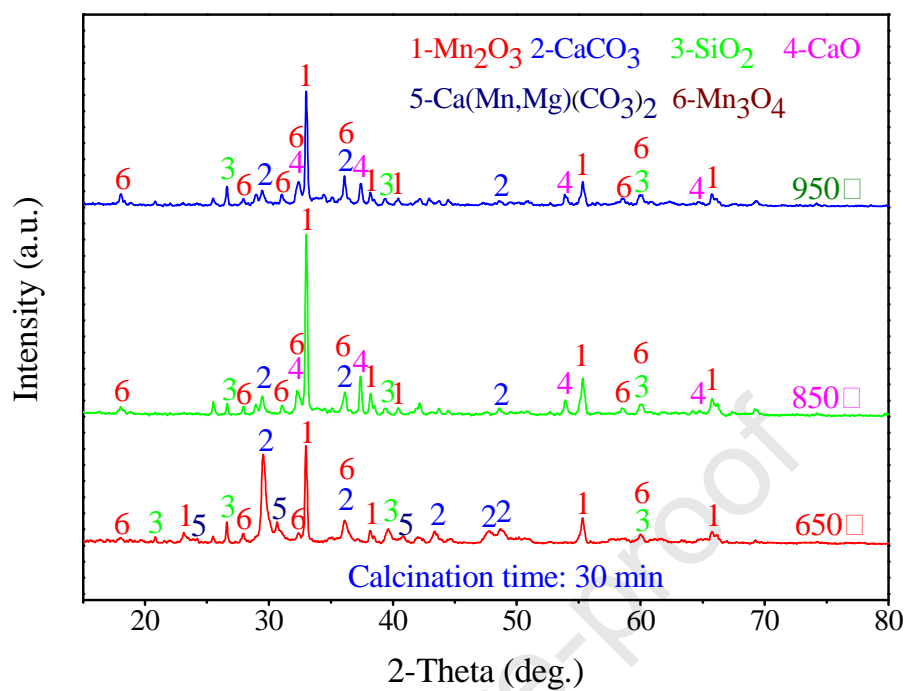
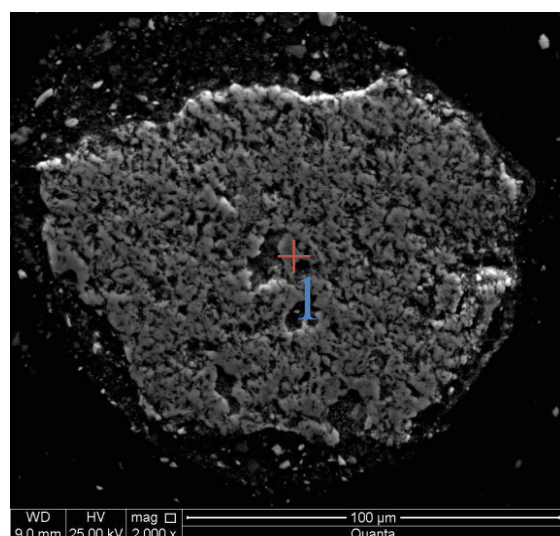
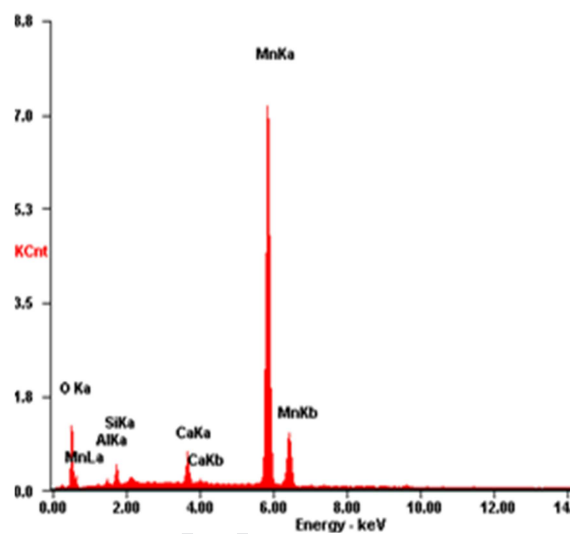


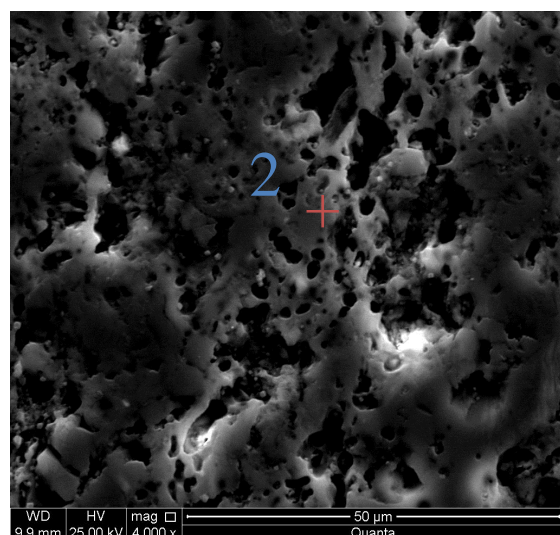
Fig. 5 XRD patterns of microwave calcined samples at different calcination temperatures.



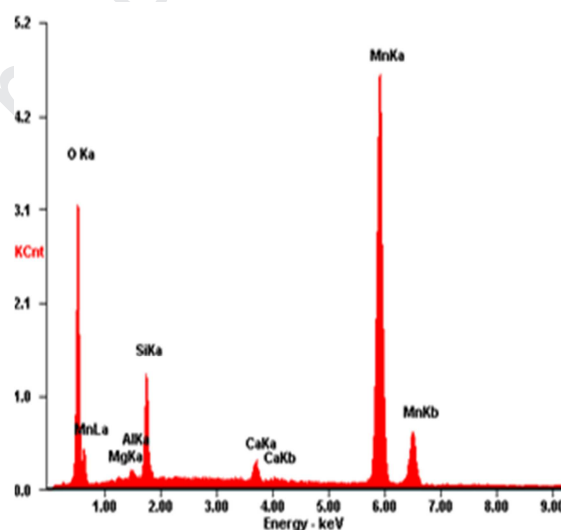
(a)



(b)



(c)



(d)

Fig. 6 SEM images and EDAX spectra of microwave calcined samples, (a) SEM of the sample calcined at 850 °C for 30 min; (b) EDAX of spot 1; (c) SEM of the sample calcined at 950 °C for 30 min; (d) EDAX of spot 2.

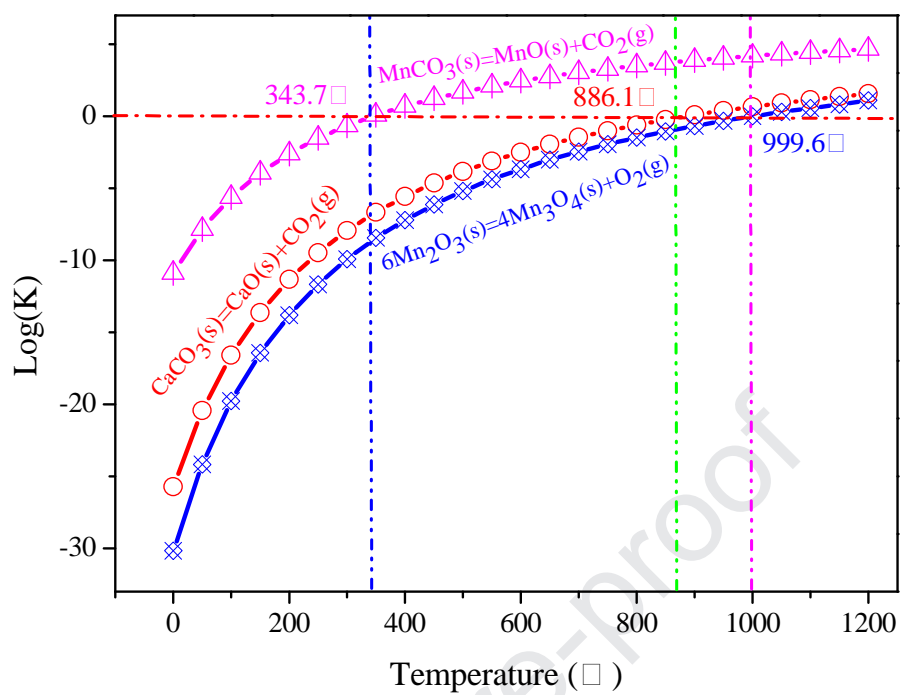


Fig. 7 Dependency of equilibrium constant on temperatures for the formation-decomposition reactions of manganese ore.

The main highlights of this work are as follows,

- (1) Exploration of dissociation behavior and thermal decomposition of manganese ore.
- (2) Microwaves as energy source to enhance dissociation behavior of manganese ore.
- (3) Manganese ore modified by microwave calcination meet industrial furnace standards.
- (4) Irregular cracks and pits appeared on surface of microwave calcined manganese ore.

Declaration of interests

☒ The authors declare that they have no known competing financial interests or personal relationships that could have appeared to influence the work reported in this paper.

☐ The authors declare the following financial interests/personal relationships which may be considered as potential competing interests: